



Micromill and in situ laser ablation sampling techniques for high spatial resolution MC-ICPMS U-Th dating of carbonates

Dirk L. Hoffmann^{a,*}, Christoph Spötl^b, Augusto Mangini^c

^a Bristol Isotope Group, School of Geographical Sciences, University of Bristol, Bristol, UK

^b Institut für Geologie und Paläontologie, Universität Innsbruck, Innsbruck, Austria

^c Heidelberger Akademie der Wissenschaften, Heidelberg, Germany

ARTICLE INFO

Article history:

Received 15 February 2008

Received in revised form 14 October 2008

Accepted 14 November 2008

Editor: B. Bourdon

Keywords:

Laser ablation

Micromill

MC-ICPMS

U-Th dating

Carbonates

ABSTRACT

Procedures for accurate determinations of ^{230}Th - ^{234}U - ^{238}U isotope ratios using in situ laser ablation (LA) and micromill techniques for carbonates such as speleothems and corals are presented. For LA analyses we use a New Wave Research UP193HE laser and a new multiple ion counting detector system available for the ThermoFinnigan Neptune MC-ICPMS. Multiple ion counting increases the efficiency of low level ion beam collection by allowing simultaneous collection of all ion beams and also circumvents problems associated with unstable, transient beams. We present results of LA U-series measurements on a U-rich (10–168 $\mu\text{g/g}$) speleothem from Spannagel Cave (Austria) and of small sub-samples from the same speleothem section prepared using a New Wave Research MicroMill and processed through separation and purification solution chemistry. Using a secular equilibrium speleothem with U concentration of 0.25 $\mu\text{g/g}$ we demonstrate that LA measurements yield accurate results on speleothem samples with less than 0.5 $\mu\text{g/g}$ U. For LA results, we currently obtain $^{230}\text{Th}/^{238}\text{U}$ results with precisions of 2% (95% confidence limit) for single isotope ratio measurements on a U-rich sample. On the low U (0.25 $\mu\text{g/g}$ U) sample we achieve a precision between 10 and 20% for single $^{230}\text{Th}/^{238}\text{U}$ measurements. Precisions of 1% and 5% ($2\sigma_m$) can be achieved for high and low U concentration samples, respectively, using 10–15 measurements on coeval sub-samples. 0.4 mg micromill sub-samples of the low U concentration sample yield $^{230}\text{Th}/^{238}\text{U}$ isotope ratios with precisions of 2%. Accuracy of LA and micromill measurements is assessed by comparison with MC-ICPMS and TIMS measurements on larger sub-samples.

Key advantages of our LA technique are, for example, high spatial resolution analyses and the possibility of rapid determination of numerous coeval sub-samples. The results on micromill samples are more precise but this sample preparation technique is time consuming and larger sample sizes than used for LA are needed for individual measurements.

© 2008 Elsevier B.V. All rights reserved.

1. Introduction

Speleothems are important terrestrial climate archives that form in karst areas in almost all parts of the world. The time resolution of the palaeoclimate proxies depends on the growth rate and analytical spatial resolutions. Hence, there is an increasing demand for higher spatial resolution of proxy measurements and U-Th dating of speleothems to investigate timing and duration of climate events like D/O cycles or Heinrich events in more detail or determine rates of changes at higher precision. Micro-sampling techniques such as micromilling or laser ablation (LA) are promising to measure e.g. U-Th isotopes on very small quantities. Previous studies demonstrated potential of micromill sampling e.g. for Sr isotope (Charlier et al., 2006) or stable

isotope measurements (Frappier et al., 2002; Spötl and Matthey, 2006). The potential and limitations of in situ laser ablation (LA) multi collector inductively coupled plasma mass spectrometry (MC-ICPMS) for U-series isotopes have been highlighted by Stirling et al. (2000) and more recently by Potter et al. (2005) and Eggins et al. (2005). However, accurate LA U-Th isotope measurements on carbonates especially with U concentrations smaller than 1 $\mu\text{g/g}$ are difficult due to small ion beams, instrumental biases and matrix dependent differences in elemental fractionation caused, for example, by laser-matrix interaction.

MC-ICPMS measurements of very small sample sizes either in situ with LA or using micromill samples pose considerable analytical challenges. We use a high U concentration calcite sample from Spannagel cave (SPA 59; Holzkämper et al., 2005) to investigate applicability, accuracy and precision of LA and micromill sampling for U-Th dating. We demonstrate that in situ LA MC-ICPMS U-Th dating can be reliably applied to carbonate samples. The precision that can be achieved depends on the U concentration and the age of the sample, i.e. the ^{230}Th

* Corresponding author. Tel.: +44 117 9289111; fax: +44 117 9287878.

E-mail addresses: dirk.hoffmann@bristol.ac.uk (D.L. Hoffmann),

christoph.spoetl@uibk.ac.at (C. Spötl), augusto.mangini@iup.uni-heidelberg.de (A. Mangini).

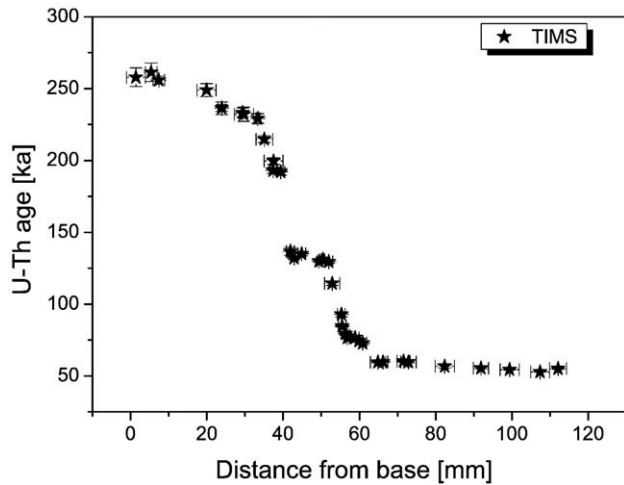


Fig. 1. TIMS U-Th dating results along the 11 cm long growth axis of flowstone SPA 59 (Holzkämper et al., 2005).

beam intensity. We investigate applicability of our LA methods on an aragonite coral sample and on speleothem carbonate with U concentration of less than $1 \mu\text{g/g}$ by comparison of the results to conventionally obtained MC-ICPMS and TIMS results at lower spatial resolution.

2. Experimental

2.1. Samples

For this study we analysed flowstone SPA 59 from Spannagel cave (Zillertal Alps, Austria) and another alpine speleothem (ERW) from Eisriesenwelt cave (Tennengebirge, Austria). Both speleothem samples consist of low-Mg calcite. Previous U-Th measurements on SPA 59 were published by Holzkämper et al. (2005) and Hoffmann (2008). The TIMS U-Th chronology for SPA 59 is based on 37 samples of 50–200 mg taken along the 11 cm thick growth section (Holzkämper et al., 2005). The flowstone formed between 260 and 55 ka mostly during the warm phases of Marine Isotope Stages (MIS) 7, 5 and 3. There is a distinct 55 ka long hiatus between the end of MIS 7 and the start of MIS 5e (Fig. 1). SPA 59 has exceptionally high U concentrations between 10 and $168 \mu\text{g/g}$ and negligible ^{232}Th making it an ideal sample for a high resolution study using very small sample sizes.

The stalagmite sample ERW from Eisriesenwelt cave has reached U-Th secular equilibrium and is thus older than 600 ka. The sample is supposed to be of pre-Pleistocene age based on oxygen and carbon isotope ratios which indicate moderate climate. U/Pb dating was not successful due to the low U contents (Frisch et al., 2002).

Analysis for this study was also done on an aragonitic coral sample WR 129 collected on Barbados. It is a coral *Acropora palmata*, taken from the same coral unit as samples UWI-2 (Gallup et al., 1994) and UWI-101 (Gallup et al., 2002). This unit has an age of 129.1 ± 0.5 (Gallup et al., 2002). TIMS measurements on WR 129 were done in the Heidelberg Academy of Science U-Th laboratory.

Table 1

Cup configuration used for LA MIC-MC-ICPMS measurements

#	IC2	IC3	IC4	IC5	IC6	L4	L3	L2	IC1	H1	H2	H4
1	228	^{230}Th	$(^{232}\text{Th})^*$	233	^{234}U	^{235}U	^{238}U					
2		230.5		233.5	234.5							
3								^{232}Th	^{234}U	^{235}U	^{238}U	
4									^{230}Th			^{238}U

MIC are IC 2–6; IC1 is the SEM in the central axis position located behind an RPQ (see text for details). (* only activated if $^{232}\text{Th} < 20$ kcps).

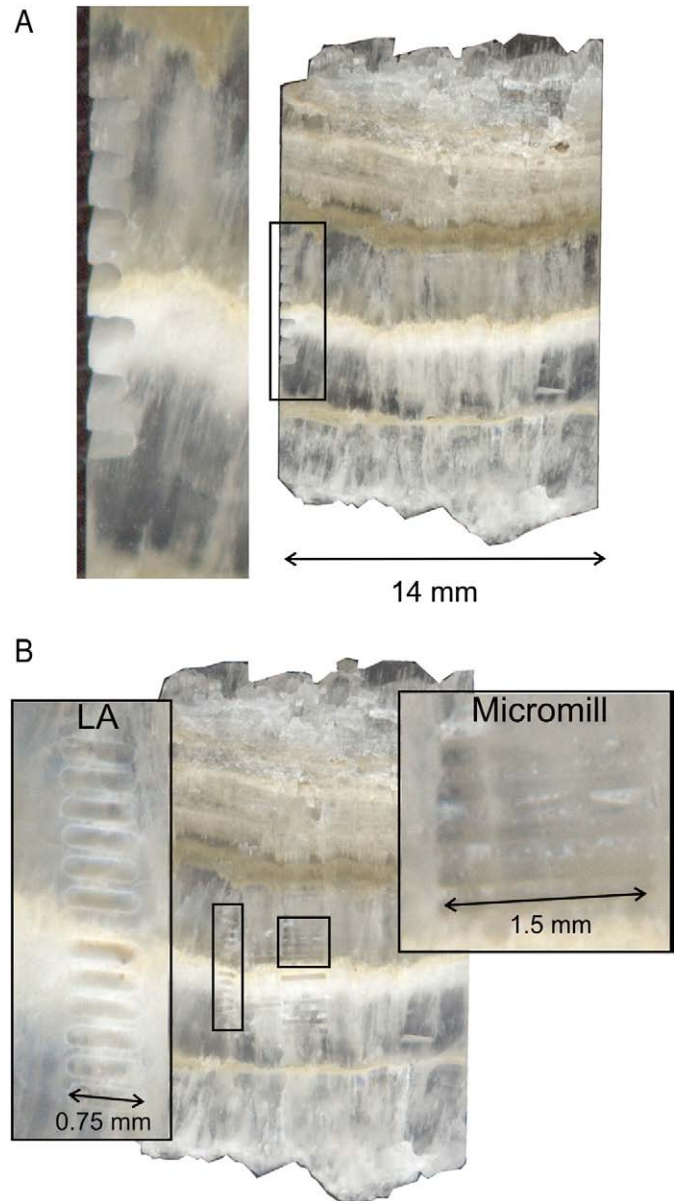


Fig. 2. A: Surface of a 1 mm thin slice of SPA 59 (1.4 cm \times 2 cm) covering the MIS 7-5 hiatus. Enlarged are the wire saw cuts for U-Th sub-sampling. The small pieces between the cuts were stripped off with a razor blade after cleaning the slice. Sample sizes were ~ 1 mg. B: Micromill and laser ablation tracks on the same slice as shown in Fig. 2A. Enlarged on the left hand side are the LA tracks (0.75 mm \times 0.25 mm) and on the right hand side the micromill tracks (1.5 mm \times 0.25 mm).

2.2. MC-ICPMS

All MC-ICPMS measurements were performed in the Bristol Isotope Group (BIG) laboratory using a ThermoFinnigan Neptune equipped with a multi ion counter (MIC) array. The MIC array in the Neptune used for LA U-Th measurements consists of 5 miniaturised channeltron ion counters, installed on the low mass side fixed to Faraday cup L4 (Table 1). The ion counter spacing is optimised for heavy isotope measurements, specifically U-Pb applications. They are set to statically measure low level ion beams of masses 202 - 204 - 206 - 207 - 208, however, using the ion optics of the Neptune the same array can be used to measure ^{230}Th and ^{234}U simultaneously on two of the ion counters (IC3-IC6) together with ^{232}Th on IC4 and ^{235}U and ^{238}U on Faraday cups. The ablation background is measured simultaneously on masses 228 and 233 and additionally on half masses 230.5, 233.5 and 234.5 during an extra LA pass. In the case of ^{232}Th beam intensities

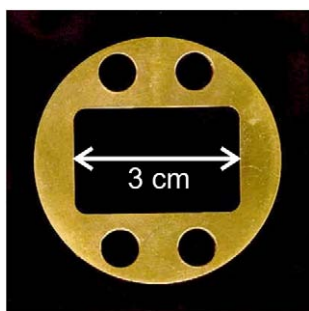


Fig. 3. Sample holder design for LA analysis.

exceeding 20 kcps we do not use a miniaturized channeltron to measure it. In this case we measure ^{232}Th either on the secondary electron multiplier (SEM) in the centre position or on a Faraday cup. In this case ^{230}Th and ^{234}U are measured with a peak jump routine on the centre SEM which is located behind an energy and angular filtering device (retarding potential quadrupole – RPQ) (Table 1). All results presented in this study were measured on samples with negligible ^{232}Th intensities thus using the MIC cup configuration. Further details about solution U-series and MIC procedures are presented in Hoffmann et al. (2007) and Hoffmann (2008). All errors quoted in this study are at the 95% confidence level, unless otherwise stated.

2.3. Diamond wire saw and micromill sample preparation

A 1 mm thick slice was cut off from flowstone SPA 59 (Holzkämper et al., 2005) for further high spatial analysis (Fig. 2A MC-ICPMS U-Th measurements were undertaken on 9 sub-samples along 7 mm of growth covering a white layer marking the MIS 7/5 hiatus. The sub-samples were cut with a spacing of 0.8 mm using a Well diamond coated wire saw at BIG (Fig. 2A). The sample slice with the wire saw cuts was cleaned in a MQ ultrasound bath to remove potential surface contamination. The small pieces were then stripped off the slice with a razorblade and weighed using a Mettler MT5 microbalance before processing through U-Th separation and purification chemistry (Hoffmann, 2008). The sample masses were around 1 mg, 6 of the U-Th results were previously reported in Hoffmann (2008) and 3 additional samples were prepared for this study.

Micro-samples with masses of about 0.09–0.1 mg were milled from the same piece of SPA 59 using a New Wave Research MicroMill. Micromill procedures were similar to those outlined in Charlier et al. (2006) for Sr isotope measurements on micro-samples. We used a Brasseler tungsten carbide mill bit with a conical shape (30-degree tip angle). The sample surface area was removed and discarded with a first pass of milling a raster of parallel tracks (10 μm deep with 5 μm spacing). For one U-Th sample we then milled 2 parallel overlapping tracks of 1.5 mm length with a 100 μm offset and each track 250 μm deep in the centre. The milled volume is about 0.044 mm^3 giving a maximum sample size of 0.12 mg. Each sample was milled in 10 passes by successively increasing the depth by 25 μm . For each pass a drop of MQ water was placed on the sample surface and milling was done in water. MQ and milled powder were taken off after each pass using a polyethylene tubing (inner diameter 0.76 mm) cut at a 45° angle at the tip and a Hamilton gastight syringe. With an estimated recovery of 80% the sample masses were calculated to be 90–100 μg . Due to unknown exact sample masses the U concentrations of micromill samples cannot be determined accurately, however, this has no significant effect on the measured isotope ratios. We milled 4 samples below and 5 samples above the white layer (Fig. 2B) with an offset of 350 μm . One sample was milled from the white layer. The procedural blank of the micromill sample preparation was assessed by consecutively placing 10 MQ water drops on the calcite surface for a similar duration as the milling process. The MQ drops are collected in the

same way as the sample drops and analysed for U- and Th isotopes. Blanks of the micromill sampling procedure are slightly elevated compared to pure analytical blanks (5 pg of ^{238}U compared to 2 pg and 2 pg of ^{232}Th compared to 1 pg).

The micromill sampling technique was also applied to the stalagmite sample from Eisriesenwelt cave. Here, we milled 4 parallel overlapping tracks of 3 mm length 100 μm apart for one U-Th sample due to smaller U concentrations expected for this sample. The sample size was calculated to be in the range of 0.4 mg. Furthermore, we cut a sample from this stalagmite (~150 mg) and another sample from the coral sample WR 129 (~70 mg) using the wire saw for conventional MC-ICPMS analyses. Chemical separation and purification of wire saw and micromill samples were done according to Hoffmann (2008). The U and Th fractions of small sub-samples were analysed on the (MIC-) MC-ICPMS as outlined in Hoffmann (2008).

2.4. Laser ablation

The LA analyses were performed using a New Wave Research UP193HE ArF Excimer laser system at BIG. The laser system has a wavelength of 193 nm and a typical power density of 5 J/cm^2 at 70% power output. The chosen laser repetition rate and the spot size depend on the U and Th concentrations. For U-Th isotope measurements we usually use a 7 Hz repetition rate and 180–250 μm spot size. For the data presented in this study we used 250 μm spot to achieve the same spatial resolution for laser and micromill samples. He is used as the ablation carrier gas, it is mixed with the Ar sample gas and N_2 in a quartz mixing cell and the mixture is then directly injected into the Ar plasma. We use a standard New Wave Research LA cell with dedicated sample holders. The sample holder design used for the analysis presented in this study is shown in Fig. 3. It consists of a central sample position with a maximum dimension of 2 \times 3 cm and 4 positions for standards with a diameter of 0.7 mm. Samples are either mounted in epoxy resin or placed on dedicated resin blocks that fit in the sample holder. One standard position is used for pieces of NIST 610 and NIST 612 glass mounted in epoxy resin. Usually two positions are used for pieces of a calibration calcite standard. One of the calcite standard pieces is placed as close as possible to the sample ablation position. Unused positions are blocked with dedicated epoxy resin blocks.

Instrumental tuning and performance checks of the Neptune MC-ICPMS are initially performed using a NBL-112a U-solution as outlined in Hoffmann et al. (2007). A uraninite solution with ^{230}Th - ^{234}U - ^{238}U isotopes is used for the specific MIC-Faraday cup configuration performance

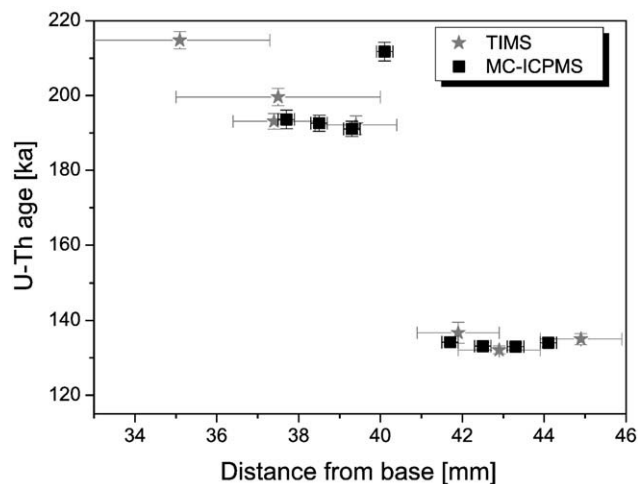


Fig. 4. MC-ICPMS U-Th results on 1 mg samples cut from SPA 59 slice (Fig. 2A) compared to TIMS results (Holzkämper et al., 2005).

Table 2
Solution U–Th results on samples SPA 59, ERW and WR 129

Lab ID	Sample ID	Distance from base [mm]	^{238}U [ng/g]	^{232}Th [ng/g]	$(^{230}\text{Th}/^{232}\text{Th})_A$	$(^{230}\text{Th}/^{238}\text{U})_A$	$(^{234}\text{U}/^{238}\text{U})_A$	U–Th age [ka]	$(^{234}\text{U}/^{238}\text{U})_{A0}$
BIG-UTH-A381	SPA59-37.7	37.70±0.10	116214±1930	1.37±0.05	235250±7150	0.906±0.004	1.074±0.002	193.6±2.5	1.128±0.003
BIG-UTH-A382	SPA59-38.5	38.50±0.10	73044±851	2.54±0.06	80100±1450	0.912±0.003	1.082±0.002	192.6±2.1	1.141±0.003
BIG-UTH-A346	SPA59-39.3	39.30±0.10	63866±280	n.d.	n.d.	0.919±0.003	1.091±0.002	191.3±1.8	1.156±0.003
BIG-UTH-A347	SPA59-40.1	40.10±0.10	38942±169	n.d.	n.d.	0.956±0.003	1.093±0.002	212.1±2.4	1.169±0.003
BIG-UTH-A348	SPA59-40.9	40.90±0.10	13557±68	49.15±0.38	984±5	1.167±0.005	1.074±0.003		
BIG-UTH-A349	SPA59-41.7	41.70±0.10	134259±570	41.17±0.32	7697±39	0.772±0.003	1.078±0.002	134.2±1.0	1.114±0.002
BIG-UTH-A350	SPA59-42.5	42.50±0.10	96983±435	n.d.	n.d.	0.778±0.003	1.089±0.002	133.2±1.0	1.129±0.002
BIG-UTH-A351	SPA59-43.3	43.30±0.10	63804±270	n.d.	n.d.	0.780±0.003	1.092±0.002	133.1±1.0	1.134±0.002
BIG-UTH-A383	SPA59-44.1	44.10±0.10	56953±615	12.49±0.17	11040±80	0.792±0.003	1.103±0.002	134.0±1.2	1.151±0.003
BIG-UTH-A93	ERW		254±2	0.07±0.00	11410±580	0.999±0.003	0.999±0.003		
BIG-UTH-A201	WR129		3179±12	0.55±0.00	13990±130	0.788±0.005	1.110±0.002	130.7±1.6	1.160±0.003
BIG-UTH-A375	SPA59-38.6-MM	38.60±0.05	62375±29717	1.13±0.49	154170±21470	0.912±0.004	1.087±0.002	189.5±2.5	1.149±0.003
BIG-UTH-A374	SPA59-38.95-MM	38.95±0.05	80515±52300	n.d.	n.d.	0.924±0.004	1.091±0.002	194.4±2.5	1.157±0.003
BIG-UTH-A373	SPA59-39.3-MM	39.30±0.05	75221±15482	17.03±3.55	12300±590	0.911±0.005	1.092±0.003	186.4±3.2	1.156±0.004
BIG-UTH-A376	SPA59-39.6-MM	39.60±0.05	47977±20096	3.66±2.15	36710±1810	0.916±0.004	1.092±0.002	189.4±2.2	1.156±0.003
BIG-UTH-A377	SPA59-40.7-MM	40.70±0.05	19177±3656	68.94±13.32	933±15	1.098±0.008	1.077±0.004	515.7±87.1	1.329±0.072
BIG-UTH-A378	SPA59-41.5-MM	41.50±0.05	129926±25838	41.99±8.31	7204±156	0.762±0.004	1.073±0.002	132.2±1.4	1.106±0.003
BIG-UTH-A366	SPA59-41.9-MM	41.90±0.05	154101±28957	187.42±39.17	1927±16	0.767±0.003	1.081±0.002	131.8±1.3	1.117±0.003
BIG-UTH-A367	SPA59-42.25-MM	42.25±0.05	115376±23794	18.05±3.80	15050±320	0.771±0.004	1.089±0.003	130.7±1.4	1.129±0.004
BIG-UTH-A368	SPA59-42.6-MM	42.60±0.05	62899±13068	4.06±0.80	36580±2890	0.772±0.004	1.086±0.003	131.8±1.4	1.125±0.004
BIG-UTH-A369	SPA59-42.95-MM	42.95±0.05	70104±14039	12.00±2.46	13800±580	0.773±0.004	1.087±0.003	132.1±1.6	1.126±0.004
BIG-UTH-A379	ERW-MM		288±60	n.d.	n.d.	1.010±0.019	0.993±0.010		

MM on the sample ID indicates micromill samples. Analytical errors are at 95% confidence level. All ratios are activity ratios, indicated by subscript A. Decay constants are $9.1577 \times 10^{-6} \text{ yr}^{-1}$ for ^{230}Th , $2.826 \times 10^{-6} \text{ yr}^{-1}$ for ^{234}U (Cheng et al., 2000), and $1.55125 \times 10^{-10} \text{ yr}^{-1}$ for ^{238}U (Jaffey et al., 1971). ^{232}Th concentration is small for all samples and no correction for detrital ^{230}Th was applied.

check. The sample introduction is then switched to the laser system and gas flows (He, Ar sample gas, N_2) are tuned using the NIST 612 glass standard and a ^{238}U beam and the cup configuration #3 and #4 (Table 1). The machine and laser tuning is finally optimised for carbonate analyses using an internal calcite standard which is also used for sample bracketing and cup configuration #1. With 180 μm spot size, 7 Hz repetition rate and 5 J/cm^2 we typically obtain a ^{238}U intensity of 1 V on the calcite standard which has a U concentration of 20 $\mu\text{g}/\text{g}$. The ^{230}Th and ^{234}U intensities are in the range of 400 and 3000 cps, respectively. We obtain an efficiency of about 0.3% for the total ablated U. The sample measurements are done following a standard-sample-standard bracketing procedure. Potential fractionation effects related to the geometry of the ablation cell are monitored using calibration standard measurements in two different positions in the cell. In the case of observed differences of the measured isotope ratios due to laser cell positions the tuning procedure is repeated and, if necessary, the sample and standard positions in the cell are rearranged. Data were only collected in the case of negligible differences between two standard positions.

A typical measurement sequence consists of background intensity measurements without ablating followed by measurements of the calcite standard in two positions in the cell. Background intensities without ablating are found to be negligible. One or two samples are then commonly analysed followed by background and standard measurements. A standard or sample analysis is usually done on a 0.5 mm long track, ablated by moving the laser spot at a speed of 20 $\mu\text{m}/\text{s}$ along the track. The beam intensity, peak shape and $^{232}\text{Th}/^{238}\text{U}$ ratio are checked on the first pass and the U–Th data collection is started on the second pass after the surface is ablated. The U–Th isotopes are measured during the following 4 passes and after that the intensities at half masses are measured on a further pass to determine laser background intensities. Background including tail contribution is interpolated for ^{230}Th and ^{234}U and subtracted from the measured intensities offline. We typically run a total 5–6 passes with a total of 2.5 min ablation time. We chose 25 cycles of 4 s integration time for the static measurement of $^{230}\text{Th} - ^{234}\text{U} - ^{235}\text{U} - ^{238}\text{U}$. In case of a ^{230}Th intensity smaller than 10 cps we increase the measurement time to a maximum of 50 cycles running up to 10 laser passes.

Ion counter dead time and dark noise as well as the Faraday cup baseline are corrected online, all other instrumental bias corrections are conducted offline. First we correct for background intensities and

ion counter linearity, then mass fractionation and ion counter gain (yield) is corrected using a correction factor derived from the measured $^{230}\text{Th}/^{238}\text{U}$ and $^{234}\text{U}/^{238}\text{U}$ isotope ratios of the bracketing secular equilibrium standard.

All laser sample surface areas were polished and cleaned (MQ ultrasound, methanol ultrasound) prior to the analysis. SPA 59 LA analyses were done on the same piece as used for conventional sampling and micromill work (Fig. 2B). 12 individual LA U–Th analyses as described above were done across the MIS 7/5 hiatus (Fig. 2B), 3 of the analyses were done below, 3 within and 6 above the white band. 10 repeat analyses of coeval samples within one layer were measured just above the white layer. We also conducted U–Th isotope measurements while moving the laser spot at 5 $\mu\text{m}/\text{s}$ along a 6 mm track across the hiatus. We integrated U–Th isotope ratios for 8 s ablation time corresponding to an average of 40 μm . The coral sample WR 129 and the Eisriesenwelt speleothem sample were also repeatedly analysed using the same LA measurement setup.

High resolution U concentration measurements using the *in-situ* LA technique were conducted on sample SPA 59 using the same New

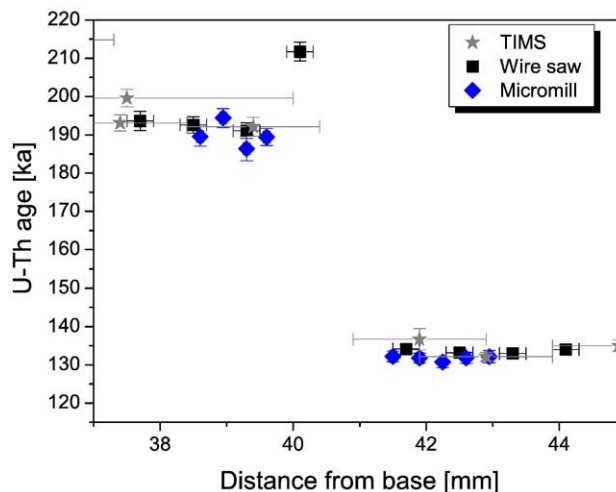


Fig. 5. MC-ICPMS U–Th results on micromill samples taken from SPA 59 (sample size ~0.1 mg) compared to the results shown in Fig. 4.

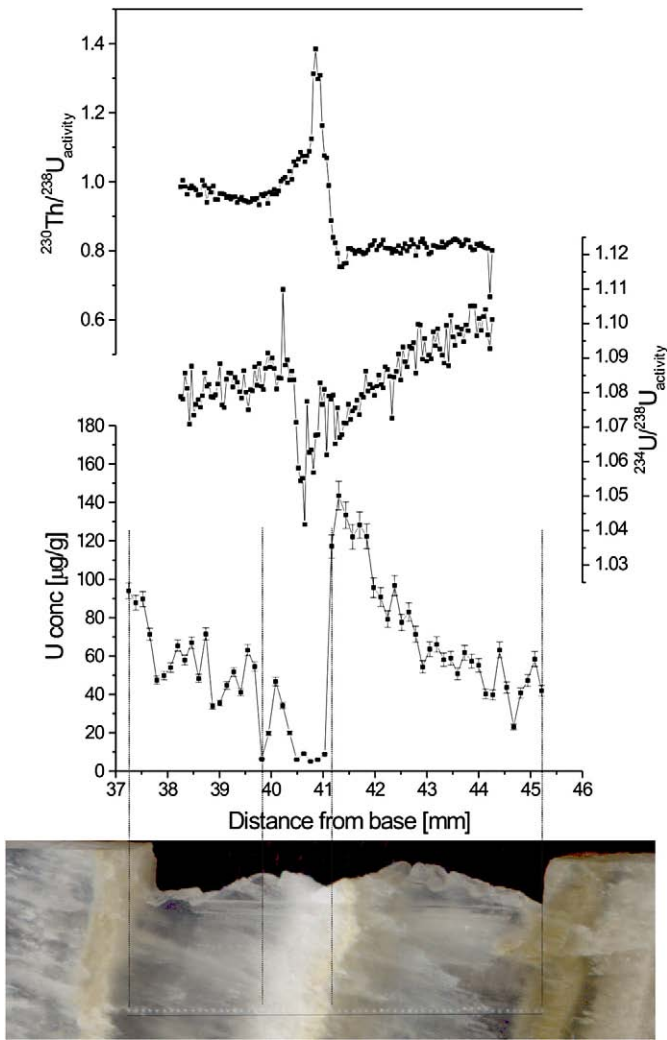


Fig. 6. LA U concentration measurements and continuous U-Th isotope scan on SPA 59. Small dots above the horizontal black line at the bottom are the LA pitches for U concentration measurements. (For interpretation of the references to colour in this figure legend, the reader is referred to the web version of this article.)

Wave Research UP193HE ArF Excimer laser system coupled to a ThermoFinnigan Element 2 sector field (SF) ICPMS at BIG following methods outlined in Hoffmann et al. (2008). Here we used single spots of 30 μm diameter. A measurement cycle consists of 40 s background and 60 s ablation measurements. The calibration standard was NIST 612 glass using the concentration values of Pearce et al. (1997). Data for LA trace element concentration measurements were reduced using the Glitter software (van Achterbergh et al., 2001). For calculation of the U concentration in the calcite sample the internal CaO was assumed to be 55 ± 2 wt.%.

3. Results

3.1. SPA 59

3.1.1. MC-ICPMS measurements on wire saw samples

For this study we focused on determining the timing of the growth stop at the end of MIS 7 and the restart of speleothem formation at the beginning of MIS 5e. Fig. 2 shows the section of SPA 59 used for the analysis. A milky-white calcite layer separates two transparent calcite layers that formed around 192 ka and 135 ka, respectively (Holzkämper et al., 2005). MC-ICPMS U-Th ages of the samples cut with the diamond wire saw (Hoffmann, 2008) indicate that the white layer was diagenetically altered probably during the 55 ka long hiatus. In

addition to the results presented in Hoffmann (2008) we prepared 3 more MC-ICPMS samples with the wire saw, the results of which are shown in Fig. 4 and Table 2. We use these MC-ICPMS U-Th results to assess the reliability of micromill and LA techniques in sections 3.1.2 and 3.1.3.

MC-ICPMS results confirm earlier TIMS results and show that the 2 mm flowstone below the white layer formed between 193.6 ± 2.5 and 191.1 ± 2.0 ka, i.e., at the end of MIS 7. Directly above the white layer we obtained ages of 134.2 ± 1.0 to 133.1 ± 1.0 ka which constrain the restart of calcite deposition at the beginning of MIS 5e consistent with Holzkämper et al. (2005) and other speleothem samples from this cave (Spötl et al., 2007). However, two results of samples taken from the white layer between 40 and 41 mm are not in stratigraphic order, one is apparently too old with 211.7 ± 2.5 ka (Fig. 4), another sample did not yield a U-Th age because the $^{230}\text{Th}/^{238}\text{U}$ was too high compared to the $^{234}\text{U}/^{238}\text{U}$ to allow to calculate an age. The U concentrations of the two samples are 39 and 13.6 $\mu\text{g}/\text{g}$, respectively, which are small compared to the average of the other sub-samples (73 $\mu\text{g}/\text{g}$) suggesting the possibility of U loss to explain the apparent age overestimation. The white layer apparently represents the former surface of the flowstone which was

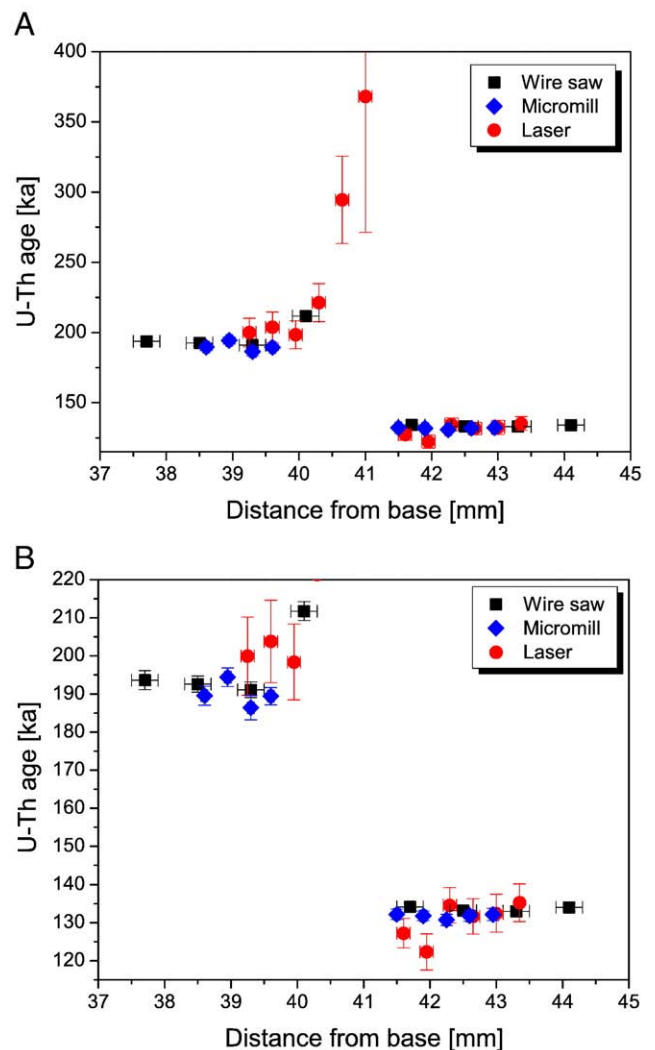


Fig. 7. A: LA-MC-ICPMS U-Th dating results on SPA 59. The results obtained on the white layer (40.5–41.4 mm) clearly demonstrate that this section cannot be dated using U-Th methods. The apparent age overestimation is a result of U loss as shown in Fig. 6. B: LA-MC-ICPMS U-Th dating results on SPA 59 below and above the white layer. (For interpretation of the references to colour in this figure legend, the reader is referred to the web version of this article.)

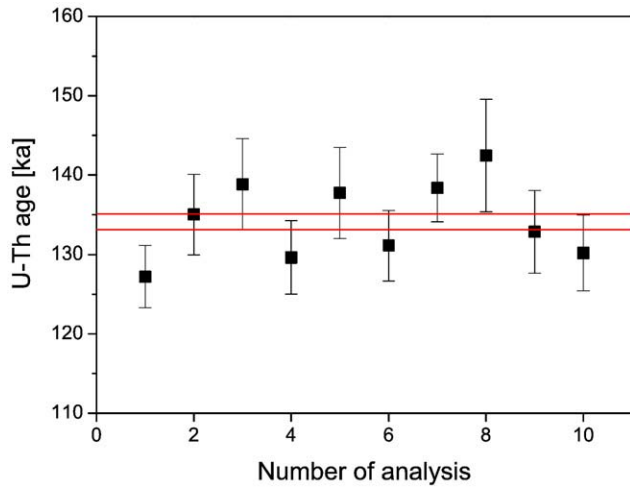


Fig. 8. Replicate LA U-Th dating measurements laterally along an individual growth layer immediately above white layer of speleothem sample SPA 59 (onset of MIS 5e calcite). The horizontal red lines indicate the 95% confidence interval of U-Th dating of the layer by solution MC-ICPMS. (For interpretation of the references to colour in this figure legend, the reader is referred to the web version of this article.)

exposed for over 55 ka. Prolonged interaction of dripwater with the topmost calcite layer might have given rise to the peculiar microcrystalline fabric and U leaching. The open system behaviour of

the white layer was not recognized by the previous TIMS analyses, only the high-resolution sampling achieved by MC-ICPMS enabled us to identify the potential problem associated with this part of the flowstone.

3.1.2. MC-ICPMS measurements on micromill samples

The same section of SPA 59 was analysed at even higher spatial resolution using the micromill technique. Fig. 5 shows the results compared to TIMS (Holzkämper et al., 2005) and MC-ICPMS results on wire saw samples. Within the analytical uncertainties the results are in good agreement. Below the white layer we obtained ages between 194.4 and 186 ka with uncertainties of 3 ka. The results scatter around the age range of 194–191 ka obtained using wire saw samples. Above the white layer the micromill samples yield ages clustering around 132–131 ka with uncertainties of 2 ka. These are slightly younger than the results of 134–133 ka presented above but agree well within their uncertainties. The sample taken from the white layer was out of range for U-Th dating, consistent with the previous results.

The micromill data demonstrate the applicability of this sampling technique for U-Th dating of carbonates using very small sample size. Compared to the samples cut with a wire saw the micromill sample results are more variable. The reason for that might be that the micromill is currently not located in a clean laboratory environment and the very small sample sizes are more prone to (cross) contamination. Further work is planned to improve the sampling procedures using micromilling.

Table 3
Laser ablation U-Th results on samples SPA 59, ERW and WR 129

Sample ID	Distance from base [mm]	^{238}U beam intensity [V]	$(^{230}\text{Th}/^{238}\text{U})_A$	$(^{234}\text{U}/^{238}\text{U})_A$	U-Th age [ka]	$(^{234}\text{U}/^{238}\text{U})_{A0}$
SPA59-39.25	39.25±0.05	2.30±0.03	0.937±0.016	1.093±0.006	199.9±10.3	1.164±0.010
SPA59-39.6	39.60±0.05	2.08±0.03	0.948±0.019	1.098±0.006	203.8±10.8	1.174±0.011
SPA59-39.95	39.95±0.05	1.57±0.08	0.943±0.016	1.102±0.007	198.4±10.0	1.178±0.011
SPA59-40.3	40.30±0.05	1.29±0.09	0.962±0.018	1.086±0.007	221.3±13.6	1.161±0.012
SPA59-40.65	40.65±0.05	0.66±0.04	1.038±0.021	1.086±0.008	294.5±31.1	1.199±0.020
SPA59-41	41.00±0.05	0.46±0.02	1.065±0.035	1.076±0.009	368.1±96.8	1.215±0.057
SPA59-41.6#01	41.60±0.05	5.10±0.05	0.749±0.011	1.076±0.006	127.2±3.9	1.109±0.008
SPA59-41.95	41.95±0.05	4.48±0.09	0.736±0.015	1.079±0.006	122.3±4.7	1.112±0.008
SPA59-42.3	42.30±0.05	3.67±0.08	0.776±0.013	1.082±0.006	134.6±4.6	1.120±0.008
SPA59-42.65	42.65±0.05	2.87±0.08	0.777±0.014	1.094±0.006	131.6±4.6	1.136±0.008
SPA59-43	43.00±0.05	2.50±0.08	0.775±0.014	1.088±0.006	132.4±5.0	1.127±0.009
SPA59-43.35	43.35±0.05	2.07±0.07	0.782±0.014	1.086±0.006	135.2±4.9	1.126±0.009
SPA59-41.6#02	41.60±0.10	2.03±0.03	0.773±0.014	1.076±0.006	135.0±5.1	1.112±0.008
SPA59-41.6#03	41.60±0.10	1.93±0.03	0.787±0.016	1.080±0.007	138.8±5.7	1.118±0.008
SPA59-41.6#04	41.60±0.10	1.96±0.01	0.751±0.013	1.069±0.006	129.6±4.6	1.100±0.008
SPA59-41.6#05	41.50±0.15	5.00±0.24	0.785±0.016	1.081±0.004	137.7±5.7	1.119±0.006
SPA59-41.6#06	41.60±0.15	6.74±0.04	0.774±0.014	1.092±0.004	131.1±4.4	1.134±0.006
SPA59-41.6#07	41.80±0.15	6.06±0.07	0.784±0.012	1.078±0.004	138.4±4.3	1.115±0.005
SPA59-41.6#08	41.50±0.15	4.77±0.16	0.792±0.019	1.074±0.004	142.4±7.1	1.110±0.006
SPA59-41.6#09	41.50±0.15	3.39±0.05	0.766±0.015	1.076±0.006	132.8±5.2	1.110±0.008
SPA59-41.6#10	41.80±0.15	3.15±0.02	0.758±0.014	1.076±0.006	130.2±4.7	1.110±0.008
ERW#01	–	0.0071±0.0002	1.081±0.214	0.947±0.040		
ERW#02	–	0.0086±0.0001	0.963±0.089	0.987±0.051		
ERW#03	–	0.0092±0.0001	0.897±0.116	0.960±0.051		
ERW#04	–	0.0086±0.0001	1.041±0.115	0.976±0.035		
ERW#05	–	0.0058±0.0001	0.966±0.091	0.959±0.040		
ERW#06	–	0.0058±0.0001	1.062±0.178	1.037±0.048		
ERW#07	–	0.0104±0.0003	0.913±0.091	0.992±0.030		
ERW#08	–	0.0084±0.0004	1.079±0.079	0.992±0.033		
ERW#09	–	0.0092±0.0002	0.875±0.111	0.953±0.038		
ERW#10	–	0.0098±0.0002	1.099±0.076	1.000±0.025		
WR129#01	–	0.123±0.001	0.762±0.030	1.112±0.013	122.8±9.2	1.158±0.018
WR129#02	–	0.096±0.002	0.796±0.033	1.111±0.017	133.0±11.2	1.162±0.023
WR129#03	–	0.111±0.001	0.786±0.033	1.097±0.012	133.6±11.3	1.141±0.017
WR129#04	–	0.099±0.002	0.809±0.028	1.110±0.013	137.6±10.0	1.163±0.018
WR129#05	–	0.172±0.002	0.811±0.019	1.106±0.008	139.2±6.8	1.157±0.011
WR129#06	–	0.184±0.002	0.833±0.018	1.106±0.008	147.0±6.8	1.161±0.011
WR129#07	–	0.095±0.001	0.794±0.024	1.112±0.010	132.1±7.9	1.163±0.014
WR129#08	–	0.100±0.002	0.830±0.026	1.110±0.011	144.6±9.7	1.166±0.016
WR129#09	–	0.119±0.002	0.790±0.025	1.111±0.011	131.2±8.3	1.161±0.015

Analytical errors are at 95% confidence level. All ratios are activity ratios, indicated by subscript A. Decay constants are 9.1577×10^{-6} yr $^{-1}$ for ^{230}Th , 2.826×10^{-6} yr $^{-1}$ for ^{234}U (Cheng et al., 2000), and 1.55125×10^{-10} yr $^{-1}$ for ^{238}U (Jaffey et al., 1971).

3.1.3. Laser ablation (MC) ICPMS

LA U concentration measurements using ThermoFinnigan Element 2 single collector SF-ICPMS were obtained on single spots of 30 μm diameter and 135 μm spacing similar to the methods described in Hoffmann et al. (2008). Fig. 6 shows the variability of the U concentration across the MIS 7/5 hiatus. The lowest U concentrations were found in the white layer with concentrations as small as 5 $\mu\text{g/g}$. These are considerably smaller than the average concentration along the 8 mm long track (60 $\mu\text{g/g}$). In more detail, the U concentration drops strongly at the beginning of the white layer from ca. 55 $\mu\text{g/g}$ in the transparent calcite (end of MIS 7) down to 6 $\mu\text{g/g}$. The U concentration then increases to values of 50 $\mu\text{g/g}$ in the lower part of the white layer but drops again to values of ca. 5 $\mu\text{g/g}$ between 40.5 and 41 mm (Fig. 6). The transparent calcite above the white layer (early MIS 5e) has very high U concentration of up to 144 $\mu\text{g/g}$. The U concentration then levels down to values around 50 $\mu\text{g/g}$. The in situ U concentration measurements provide important information about the spatial distribution of U and expected intensities for isotope measurements and/or required sample sizes for micromill samples. The results also indicate that the white layer most likely suffered U loss in the areas with U concentrations less than ~ 20 $\mu\text{g/g}$.

The in situ LA ^{230}Th – ^{234}U – ^{238}U isotope ratios were initially measured along a 6 mm long track along the growth axis. Fig. 6 also shows the $^{230}\text{Th}/^{238}\text{U}$ and $^{234}\text{U}/^{238}\text{U}$ ratios continuously measured on a parallel track to the U concentration measurements. Each ratio integrates 40 μm along the track. These data are not very precise but demonstrate the spatial variability of the U and Th isotope ratios and provide information about LA intensities of the minor isotopes (^{230}Th and ^{234}U) for further analyses. MIS 7 and MIS 5 can be identified in the difference of the $^{230}\text{Th}/^{238}\text{U}$ ratios with values around 0.95 and 0.8, respectively. Very interesting is the pattern of the $^{230}\text{Th}/^{238}\text{U}$ and $^{234}\text{U}/^{238}\text{U}$ ratios in the area of the white layer. The $^{234}\text{U}/^{238}\text{U}$ activity ratio of the transparent calcite at the end of MIS 7 is fairly stable around 1.08. The $^{234}\text{U}/^{238}\text{U}$ remains unchanged in the first 0.5 mm of the white calcite and then drops significantly parallel with the second drop in the U concentration. The ratio then scatters and increases again towards the top of the white layer. There, the $^{234}\text{U}/^{238}\text{U}$ drops again and then gradually increases further upsection, i.e., in opposite direction compared to the U concentration. This pattern might indicate a change of the U source with a mixture of U from older sources ($^{234}\text{U}/^{238}\text{U}$ closer to equilibrium) at start of MIS 5e. This U pulse vanishes and the $^{234}\text{U}/^{238}\text{U}$ activity ratio increases to values of 1.08–1.10. The $^{230}\text{Th}/^{238}\text{U}$ activity ratios clearly demonstrate that the white layer cannot reliably be dated using the U–Th method. The $^{230}\text{Th}/^{238}\text{U}$ ratio increases dramatically up to 1.4 between 39.8 and 40.8 mm from bottom (Fig. 6). This value exceeds the $^{234}\text{U}/^{238}\text{U}$ ratio by far and thus strongly indicates U loss. At the upper boundary of the white layer the ratio drops from 1.4 to 0.8. This result indicates that U leaching affected the Th–U ratios in this part of the flowstone which was most likely the flowstone palaeosurface during MIS 6.

The potential of in situ LA measurements to reliably date speleothems is demonstrated using the 12 individual U–Th analyses across the MIS 7/5 boundary. The dating results are shown in Fig. 7A and B and are compared to the conventional MC–ICPMS data. The three LA results obtained within the white layer demonstrate the systematic age overestimation due to the U leaching. Fig. 7B shows the LA results for the sections below and above the white layer only. The three analyses below the white layer yielded U–Th ages of 204 ± 11 to 198 ± 10 ka, which are slightly older than the conventional U–Th data. The precision of the individual LA U–Th ages is ca 5% and within their analytical uncertainties, however, the three results are concordant with results on wire saw samples. The six analyses above the white layer largely show excellent agreement with the U–Th dating results on wire saw samples (Fig. 7B). The first two data points above the white layer are slightly too young but the following four data are in very good agreement with the U–Th dates shown in section 3.1.1 and yield ages of 134.6 ± 4.6 to 132.4 ± 5.0 ka with individual uncertainties of ca 4%.

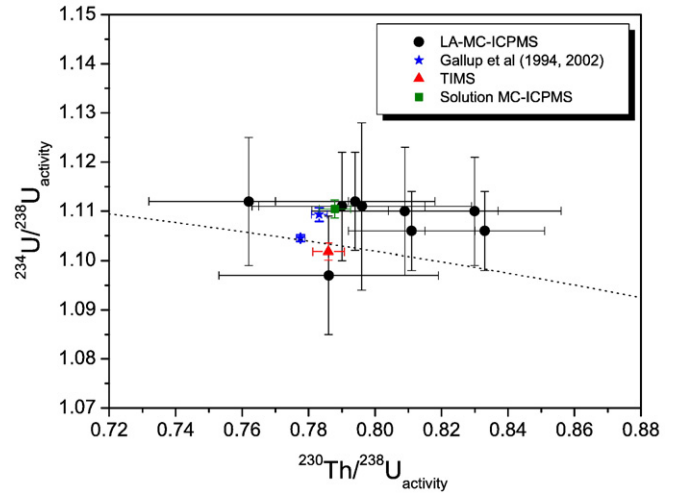


Fig. 9. LA U–Th isotope measurements on the aragonite coral sample WR 129. The $^{234}\text{U}/^{238}\text{U}$ activity ratios are plotted against the $^{230}\text{Th}/^{238}\text{U}$ activity ratios. The dotted line indicates the sea water evolution curve for initial $^{234}\text{U}/^{238}\text{U}_{\text{act}}$ of 1.15.

The apparent age underestimation of the LA U–Th measurement directly above the white layer (127.2 ± 3.9 ka) was examined in more detail. We analysed 9 additional lateral, i.e. coeval sub-samples at the same distance just above the white layer (i.e., at 41.7 ± 0.1 mm from the base) spread over the 14 mm width of the sample piece shown in Fig. 2A. Fig. 8 highlights potential and limits of in situ LA U–Th dating of carbonates. The individual age uncertainties are ca 4% and all results except two agree very well with the conventional U–Th dates of this layer. The mean age of 134.3 ± 3.1 ka ($2 \sigma_m$) is in excellent agreement with the solution MC–ICPMS derived age of 134.1 ± 1.0 ka. This shows that accurate LA U–Th isotope measurements and dating can be achieved with a precision of ca 2% ($2 \sigma_m$) if 10 or more replicate measurements are performed. The uncertainty of a single U–Th age of a high U sample is in the range of 3–5%.

3.2. Aragonite

Corals are another interesting application for in situ LA U–Th dating of carbonates. Most reef-building corals are aragonitic and have U concentrations of ca 3 $\mu\text{g/g}$. Potter et al. (2005) successfully applied the LA technique to corals using a 77 ka old coral as calibration standard. Corals are prone to diagenetic effects (e.g. Gallup et al., 1994; Scholz et al., 2004; Potter et al., 2004), however, and the isotopic composition can be inhomogeneous for a coral (Scholz and Mangini, 2007) chosen to be the standard. An LA calibration standard, however, has to be isotopically homogeneous. Thus, a secular equilibrium standard as used above would also be ideal for measurements of coral samples, but undisturbed corals in secular equilibrium are scarce. Our secular equilibrium standard is calcitic and we explore the applicability of a calcite standard for LA measurements on aragonite samples. Therefore we use the U-rich calcite secular equilibrium standard to correct the measured LA ratios of the aragonite sample WR 129 and compare to results obtained by solution MC–ICPMS and TIMS. Table 3 shows the nine individual LA results which yield mean ratios of $^{230}\text{Th}/^{238}\text{U} = 0.801 \pm 0.015$ and $^{234}\text{U}/^{238}\text{U} = 1.108 \pm 0.003$ resulting in a mean U–Th age of 135.6 ± 5.1 ka for the coral sample WR 129. The ratios measured with MC–ICPMS on a 70 mg sub-sample are $^{230}\text{Th}/^{238}\text{U} = 0.788 \pm 0.005$ and $^{234}\text{U}/^{238}\text{U} = 1.110 \pm 0.002$ with an age of 130.7 ± 1.6 (Table 2) in good agreement with dating results for the coral unit by Gallup et al. (1994, 2002). Although the LA $^{230}\text{Th}/^{238}\text{U}$ ratios agree with the conventional results within their analytical uncertainties, the slight deviation from the age given by Gallup et al. (2002) might suggest a small-scale sample inhomogeneity. Furthermore, the mean solution MC–ICPMS age is younger than a TIMS result of 132.4 ± 1.5 measured on another sub-sample in the Heidelberg

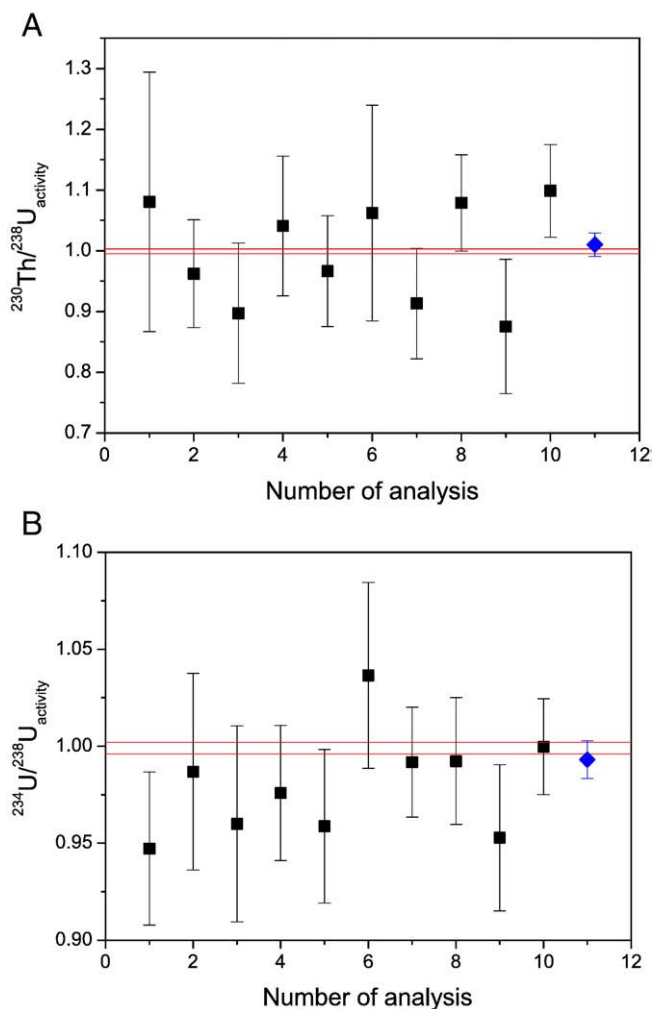


Fig. 10. A and B: LA U-Th measurements on low U (0.25 µg/g) secular equilibrium calcite ERW. The horizontal red lines indicate the 95% confidence interval of the isotope ratios obtained on a 150 mg sample measured by solution MC-ICPMS. The last data point (analysis #11) is obtained on a micromilled sub-sample (ERW-MM, Table 2). (For interpretation of the references to colour in this figure legend, the reader is referred to the web version of this article.)

laboratory but the results agree within uncertainties. The TIMS result, however, does not agree with the age of the coral unit of 129.1 ± 0.5 (Gallup et al., 2002). This also suggests minor inhomogeneities in this coral sample probably due to post depositional diagenetic effects as recently discussed by Scholz and Mangini (2007). Fig. 9 shows the $^{234}\text{U}/^{238}\text{U}$ activity ratios versus the $^{230}\text{Th}/^{238}\text{U}$ activity ratios measured by LA together with the results published by Gallup et al. (1994, 2002) and the TIMS result. The LA ratios generally fall above the sea water evolution curve which describes the temporal development of activity ratios under closed-system conditions with the initial $^{234}\text{U}/^{238}\text{U}_{\text{act}}$ of modern seawater. The measured $^{234}\text{U}/^{238}\text{U}_{\text{act}}$ are relatively constant but $^{230}\text{Th}/^{238}\text{U}_{\text{act}}$ show a large spread from 0.762 to 0.833 which indicates diagenetic alteration and U loss (or addition) as, for example, also found by Scholz et al. (2006) for corals from the same location on Barbados. However, there is no clear trend between $^{234}\text{U}/^{238}\text{U}$ and $^{230}\text{Th}/^{238}\text{U}$ as suggested by recent diagenetic models (Thompson et al., 2003; Villemant and Feuillet, 2003; Scholz et al., 2004) leaving a general applicability of any of these models in some doubt. The LA results were obtained on tracks spread over an area of about 0.5 cm^2 . Although a systematic offset of LA results due to matrix differences of aragonite and calcite cannot be excluded, the data clearly demonstrate that a single U-Th analysis would most likely not yield an accurate result. This highlights the need for multiple analyses on coeval samples for accurate

dating of reef building corals as previously discussed by Scholz and Mangini (2007). The LA technique can be used to investigate small scale variability of $^{234}\text{U}/^{238}\text{U}$ and $^{230}\text{Th}/^{238}\text{U}$ ratios in a coral sample and, where applicable, LA measurements can potentially be used to measure tightly defined isochrons for applying the correction models proposed by Scholz et al. (2004) or Villemant & Feuillet (2003).

Given that corals are commonly diagenetically altered to some extent, the requirement of a homogeneous isotopic composition is often violated. Our results indicate that matrix differences between calcite and aragonite are small and within the precision that can be achieved and a calcite standard can be used to reliably correct LA U-Th isotope measurements of an aragonite sample. This is important in the light of the difficulty to identify undisturbed secular equilibrium coral standards.

3.3. Low U calcite

We also investigated the usefulness of the techniques presented in this study for a low U concentration speleothem sample from the Eisriesenwelt cave which poses a significant analytical challenge for both LA and micromill techniques. A MC-ICPMS analysis obtained on a 150 mg sub-sample following Hoffmann et al. (2007) shows that the sample is in secular equilibrium ($^{230}\text{Th}/^{238}\text{U} = 0.999 \pm 0.004$ and $^{234}\text{U}/^{238}\text{U} = 0.999 \pm 0.003$). The U concentration is ca 0.25 µg/g which is a common value for speleothems. The micromill sample (0.4 mg) shows excellent agreement with the conventional U-Th data. Due to the very small sample size the $^{230}\text{Th}/^{238}\text{U}$ and $^{234}\text{U}/^{238}\text{U}$ ratios of 1.01 ± 0.02 and 0.993 ± 0.01 , respectively, have uncertainties in the range of 2 and 1% and are within error in secular equilibrium. The ^{238}U blank of 5 pg compared to the total U load of 100 pg is a possible reason for the slight deviation of the mean micromill results from secular equilibrium. We also measured ten coeval samples on the same sample piece using the LA method. The beam intensities were close to the limits for reliable U-Th isotope analyses (ca 5 cps for ^{230}Th , 30 cps for ^{234}U and 5–10 mV of ^{238}U) ultimately limiting the precision that can be achieved for the individual $^{230}\text{Th}/^{238}\text{U}$ and $^{234}\text{U}/^{238}\text{U}$ ratios to 10–20% and 5%, respectively. Fig. 10 shows the results of the LA measurements which scatter around the secular equilibrium value with a mean of $^{230}\text{Th}/^{238}\text{U} = 0.998 \pm 0.05$ and $^{234}\text{U}/^{238}\text{U} = 0.98 \pm 0.02$.

The results show that the LA technique described above can be used to derive accurate results on samples with U concentration smaller than 1 µg/g. They also show that the precision of in situ techniques for dating is restricted by the intensity of the ^{230}Th beam. Hence, a sample with a U concentration of e.g. 0.2 µg/g will not yield precise results unless its age is higher than ca. 100 ka.

4. Conclusions

Technical advances such as new generations of LA systems and in mass spectrometry, e.g. with the advent of multiple ion counting (MIC) arrays for the Neptune MC-ICPMS, enable U-Th isotope measurements at very high spatial resolution.

Micromill samples with U contents of 0.1 ng can be analysed with precisions of 1% for $^{234}\text{U}/^{238}\text{U}$ and 2% for $^{230}\text{Th}/^{238}\text{U}$. The precision of individual LA U-Th isotope ratio measurements currently achievable on a 0.25 µg/g U secular equilibrium sample are 3–5% for $^{234}\text{U}/^{238}\text{U}$ and 10–20% for $^{230}\text{Th}/^{238}\text{U}$. Carbonate samples with U concentrations of around 3 µg/g and 129 ka old yield precisions of 1% ($^{234}\text{U}/^{238}\text{U}$) and 3% ($^{230}\text{Th}/^{238}\text{U}$) for individual LA analyses enabling accurate and highly spatial resolved U-Th dating. The highest precision of in situ LA U-Th dating can be achieved by multiple measurements of coeval samples with a current precision limit of ca 2% ($2 \sigma_m$) on a 134 ka old sample with 134 µg/g U. To obtain accurate in situ LA results it is essential to use a matrix matching calibration standard with a well characterised, homogeneous U-Th isotopic composition. Thus, for U-Th isotope measurements on carbonates a U-rich secular

equilibrium standard is ideal. There is no significant difference between calcite and aragonite and accurate U–Th isotope ratios were obtained on a coral sample using the calcite standard for isotope ratio calibration.

The LA U–Th measurements outlined in this study are specifically designed for carbonates with low or negligible ^{232}Th concentrations. Samples with high ^{232}Th cannot be measured using the MIC array and require a setup including a Faraday cup for ^{232}Th and a secondary electron multiplier (SEM) behind the RPQ for ^{230}Th isotope measurements, operated in a peak jump mode with ^{234}U measurement on the same SEM (currently being investigated).

Micromill results are more precise than LA analysis but also much more time consuming. 10 to 15 U–Th isotope results can be measured in one day using LA. The same number of samples using the micromill technique will take at least 2 weeks. Another advantage of the in situ technique is that continuous LA isotope measurements provide a powerful tool for isotope ratio screening. This helps to identify problematic areas for U–Th dating including diagenetically altered or leached sections such as the white layer in speleothem sample SPA 59. The leaching problem of the white layer was not identified by previous TIMS analyses.

Speleothems such as stalagmites or flowstones are generally considered closed systems and thus ideally suitable for U–Th dating. However, our results demonstrate that this assumption is not a priori fulfilled for speleothem samples, especially where hiatus are present. Growth interruptions are common in many speleothems and long exposure times may lead to leaching of the surface layer if aggressive waters enter the cave system. The exact timing of a growth interruption is therefore potentially problematic to date. Highly spatially resolved sampling techniques such as LA provide a means to identify such leaching effects and to avoid sampling material from such zones.

LA and micromill U–Th measurements allow very high spatial resolution dating of palaeoclimate archives and hence can be used to determine the start and end of climate events such as the end of MIS 7 and the onset of MIS 5 or to investigate rates of climate change in detail. Furthermore, these techniques allow to analyse changes in speleothem growth rates. Microsampling techniques are also ideal to study tiny precious samples such as cave art or chondrites.

Acknowledgements

The authors wish to thank J. Kuhlemann (University of Tübingen) for the speleothem sample from Eisriesenwelt cave and C. Coath (University of Bristol) for keeping the mass spectrometers happy. The work of DLH was financially supported by the Leverhulme Trust. CS acknowledges FWF grant Y122–GEO.

References

Charlier, B.L.A., Ginibre, C., Morgan, D., Nowell, G.M., Pearson, D.G., Davidson, J.P., Ottley, C.J., 2006. Methods for the microsampling and high-precision analysis of strontium and rubidium isotopes at single crystal scale for petrological and geochronological applications. *Chemical Geology* 232, 114–133.

- Cheng, H., Edwards, R.L., Hoff, J., Gallup, C.D., Richards, D.A., Asmerom, Y., 2000. The half-lives of uranium-234 and thorium-230. *Chemical Geology* 169, 17–33.
- Eggins, S.M., Grün, R., McCulloch, M.T., Pike, A.W.G., Chappell, J., Kinsley, L., Mortimer, G., Shelley, M., Murray-Wallace, C.V., Spötl, C., Taylor, L., 2005. In situ U-series dating by laser-ablation multi-collector ICPMS: new prospects for Quaternary geochronology. *Quaternary Science Reviews* 24, 2523–2538.
- Frappier, A., Sahagian, D., González, L.A., Carpenter, S.J., 2002. El Niño events recorded by stalagmite carbon isotopes. *Science* 298, 565.
- Frisch, W., Kuhlemann, J., Dunkl, I., Székely, B., Vennemann, T., Rettenbacher, A., 2002. Dachstein-Altfläche, Augenstein-Formation und Höhlenentwicklung - die Geschichte der letzten 35 Millionen Jahre in den zentralen Nördlichen Kalkalpen. *Die Höhle* 53, 1–37.
- Gallup, C.D., Edwards, R.L., Johnson, R.G., 1994. The timing of high sea levels over the past 200,000 years. *Science* 263, 796–800.
- Gallup, C.D., Cheng, H., Taylor, F.W., Edwards, R.L., 2002. Direct determination of the timing of sea level change during termination II. *Science* 295, 310–313.
- Hoffmann, D.L., 2008. ^{230}Th isotope measurements of femtogram quantities for U-series dating using multi ion counting (MIC) MC-ICPMS. *International Journal of Mass Spectrometry* 275, 75–79.
- Hoffmann, D.L., Prytulak, J., Richards, D.A., Elliott, T.R., Coath, C.D., Smart, P.L., Scholz, D., 2007. Procedures for accurate U and Th isotope measurements by high precision MC-ICPMS. *International Journal of Mass Spectrometry* 264, 97–109.
- Hoffmann, D.L., Paterson, B.A., Jonckheere, R., 2008. Uranium concentration measurements on a fossil equid tooth by fission tracks, TIMS and laser-ablation ICPMS – implications for ESR dating. *Radiation Measurements* 43, 5–13.
- Holzkämper, S., Spötl, C., Mangini, A., 2005. High-precision constraints on timing of Alpine warm periods during the middle to late Pleistocene using speleothem growth periods. *Earth and Planetary Science Letters* 236, 751–764.
- Jaffey, A.H., Flynn, K.F., Glendenin, L.E., Bentley, W.C., Essling, A.M., 1971. Precision measurement of half-lives and specific activities of ^{235}U and ^{238}U . *Physical Review C* 4, 1889–1906.
- Pearce, N.J.G., Perkins, W.T., Westgate, J.A., Gorton, M.P., Jackson, S.E., Neal, C.R., Chenery, S.P., 1997. A Compilation of new and published major and trace element data for NIST SRM 610 and NIST SRM 612 glass reference materials. *Geostandards Newsletter* 21, 115–144.
- Potter, E.K., Esat, T.M., Schellmann, G., Radtke, U., Lambeck, K., McCulloch, M.T., 2004. Suborbital-period sea-level oscillations during marine isotope substages 5a and 5c. *Earth and Planetary Science Letters* 225, 191–204.
- Potter, E.-K., Stirling, C.H., Wiechert, U.H., Halliday, A.N., Spötl, C., 2005. Uranium-series dating of corals in situ using laser-ablation MC-ICPMS. *International Journal of Mass Spectrometry* 240, 27–35.
- Scholz, D., Mangini, A., 2007. How precise are U-series coral ages? *Geochimica et Cosmochimica Acta* 71, 1935–1948.
- Scholz, D., Mangini, A., Felis, T., 2004. U-series dating of diagenetically altered fossil reef corals. *Earth and Planetary Science Letters* 218, 163–178.
- Scholz, D., Mangini, A., Meischner, D., 2006. U-redistribution in fossil reef corals from Barbados, West Indies, and sea-level reconstruction for MIS 6.5. In: Sirocko, F., Claussen, M., Litt, T., Sánchez-Goni, M.F. (Eds.), *The Climate of Past Interglacials. Developments in Quaternary Science Series*, vol. 7, pp. 119–140.
- Spötl, C., Mathey, D., 2006. Stable isotope microsampling of speleothems for palaeoenvironmental studies: a comparison of microdrill, micromill and laser ablation techniques. *Chemical Geology* 235, 48–58.
- Spötl, C., Holzkämper, S., Mangini, A., 2007. The last and the penultimate interglacial as recorded by speleothems from a climatically sensitive high-elevation cave site in the Alps. In: Sirocko, F., Claussen, M., Litt, T., Sánchez-Goni, M.F. (Eds.), *The Climate of Past Interglacials. Developments in Quaternary Science Series*, vol. 7, pp. 471–491.
- Stirling, C.H., Lee, D.-C., Christensen, J.N., Halliday, A.N., 2000. High precision in situ ^{238}U – ^{234}U – ^{230}Th isotopic analysis using laser ablation multiple collector ICPMS. *Geochimica et Cosmochimica Acta* 64, 3737–3750.
- Thompson, W.G., Spiegelmann, M.W., Goldstein, S.L., Speed, R.C., 2003. An open-system model for U-series age determinations of fossil corals. *Earth and Planetary Science Letters* 210, 365–381.
- van Achterbergh, E., Ryan, C.G., Griffin, W.L., 2001. GLITTER version 4. Macquarie Research Ltd.
- Villemant, B., Feuillet, N., 2003. Dating open systems by the ^{238}U – ^{234}U – ^{230}Th method: application to Quaternary reef terraces. *Earth and Planetary Science Letters* 210, 105–118.